AD-A132 098 ASYMPTOTIC HIGH FREQUENCY TECHNIQUES FOR THE UHF AND ABOVE ANTENNAS(U) OHIO STATE UNIV COLUMBUS ELECTROSCIENCE LAB R G KOUYOUMJIAN ET AL. NOV 76 1/1

UNCLASSIFIED ESL-4508-1 N00123-76-C-1371 F/G 9/5 NL

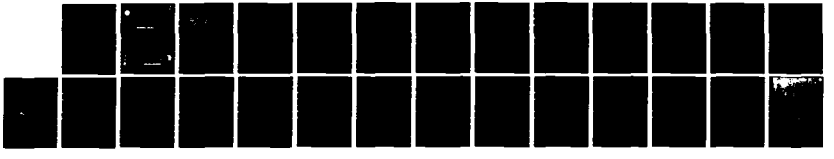

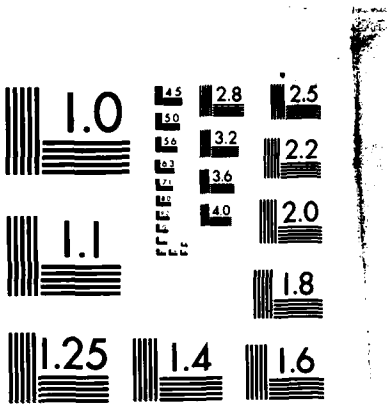

MICROCOPY RESOLUTION TEST CHART
NATIONAL BUREAU OF STANDARDS-1963-A

[redacted] HIGH FREQUENCY TECHNIQUES FOR UHF AND ABOVE ANTENNAS

[redacted] Quarterly Report - 1 August 1976 to 31 October 1976

R. G. Kouyoumjian
R. J. Marhefka
R. C. Rudduck
C. H. Walter

The Ohio State University
ElectroScience Laboratory
Department of Electrical Engineering
Columbus, Ohio 43212

Report [redacted]
Contract [redacted]
November 1976

Naval Regional Procurement Office
Long Beach, California 90822

[redacted]

NOTICES

When Government drawings, specifications, or other data are used for any purpose other than in connection with a definitely related Government procurement operation, the United States Government thereby incurs no responsibility nor any obligation whatsoever; and the fact that the Government may have formulated, furnished, or in any way supplied the said drawings, specifications, or other data, is not to be regarded by implication or otherwise as in any manner licensing the holder or any other person or corporation, or conveying any rights or permission to manufacture, use, or sell any patented invention that may in any way be related thereto.

UNCLASSIFIED

SECURITY CLASSIFICATION OF THIS PAGE *(When Data Entered)*

REPORT DOCUMENTATION PAGE	READ INSTRUCTIONS BEFORE COMPLETING FORM
1 REPORT NUMBER	2. GOVT ACCESSION NO. A192098 / 3 RECIPIENT'S CATALOG NUMBER
4. TITLE *(and Subtitle)* ASYMPTOTIC HIGH FREQUENCY TECHNIQUES FOR UHF AND ABOVE ANTENNAS	5 TYPE OF REPORT & PERIOD COVERED First Quarterly Report 8/1/76 - 10/31/76
	6 PERFORMING ORG. REPORT NUMBER ESL 4508-1
7. AUTHOR(s) R.G. Kouyoumjian, R. J. Marhefka R. C. Rudduck, C.H. Walter	8 CONTRACT OR GRANT NUMBER(s) N00123-76-C-1371
9. PERFORMING ORGANIZATION NAME AND ADDRESS The Ohio State University ElectroScience Laboratory, Department of Electrical Engineering Columbus, Ohio 43220	10. PROGRAM ELEMENT, PROJECT, TASK AREA & WORK UNIT NUMBERS Project N00953/6/009121
11. CONTROLLING OFFICE NAME AND ADDRESS Naval Regional Procurement Office Long Beach, California 90822	12 REPORT DATE November 1976 13. NUMBER OF PAGES 21
14. MONITORING AGENCY NAME & ADDRESS*(if different from Controlling Office)*	15. SECURITY CLASS. *(of this report)* Unclassified 15a. DECLASSIFICATION DOWNGRADING SCHEDULE

16. DISTRIBUTION STATEMENT *(of this Report)*

Approved for public release;
distribution unlimited.

17. DISTRIBUTION STATEMENT *(of the abstract entered in Block 20, if different from Report)*

18. SUPPLEMENTARY NOTES

19. KEY WORDS *(Continue on reverse side if necessary and identify by block number)*

Computer code	Aperture integration
Algorithm	Slope diffraction
Geometrical Theory of Diffraction	Flat plates
Far field pattern	Cylinders

20 ABSTRACT *(Continue on reverse side if necessary and identify by block number)*

The overall scope of the program on Contract No. N00123-76-C-1371 between The Ohio State University ElectroScience Laboratory and the Naval Electronics Laboratory Center is to develop the necessary theory, algorithms and computer codes for simulating antennas at UHF and above in a complex ship environment. The work consists of a) basic scattering code development, b) reflector antenna code development and c) basic studies to support items a) and b). This report describes the progress in each of these three areas for the period 1 August 1976 to 31 October, 1976.

DD FORM 1 JAN 73 1473 EDITION OF 1 NOV 65 IS OBSOLETE

UNCLASSIFIED

SECURITY CLASSIFICATION OF THIS PAGE *(When Data Entered)*

CONTENTS

I. INTRODUCTION

This report describes the work done on Contract No. N00123-76-C-1371 for the period 1 August 1976 to 31 October 1976.

The overall program is divided into three areas. These are 1) basic scattering code development, 2) reflector antenna code development and 3) basic theoretical studies to support the first two areas. The following sections describe the overall scope of effort and the progress made to date in each of the three areas mentioned above.

II. PROGRAM SCOPE

The scope of the work under Contract No. N00123-76-C-1371 is to develop the necessary theory, algorithms and computer codes for simulating antennas at UHF and above in a complex ship environment. A milestone chart for the total program, which extends over a three year period, is shown in Table I. A more detailed breakdown of the effort planned for the first year is shown in Table II. The following sections describe the progress made during the first quarter of the program in Table II.

III. BASIC SCATTERING CODE DEVELOPMENT

The purpose of this section is to describe the present status of the basic scattering code development for the analysis of antennas in a complex shipboard environment. The proposed high frequency model for a ship will eventually be composed of flat plates, box-like structures and finite elliptic cylinders that will represent the various component structures of the ship. These various structures can greatly affect the pattern performance of an antenna. The structures are being analyzed by the use of the Geometrical Theory of Diffraction (GTD) and resulting algorithms will be developed into a user oriented computer code.

The advantage of using the GTD is that the various component parts of a complex structure can be analyzed separately in a manageable form. The simple structures can then be systematically combined, being careful to include only the necessary interaction terms between scattering structures, to obtain a result that will be accurate enough for engineering purposes while still being efficient and easy to use. The GTD is also versatile enough to accommodate other solutions such as modal solutions, physical optics and moment methods to increase its capabilities.

See Table II for the first Quarter of the scattering code development program. The basic flat plate and finite elliptic cylinder structures, successfully used to model aircraft structures [1], are being modified into a form compatible with ship structures. The flat plates will be used as the flat faces of a box shape to represent structural parts of a ship. The finite elliptic cylinders will be used to represent poles, masts, etc.

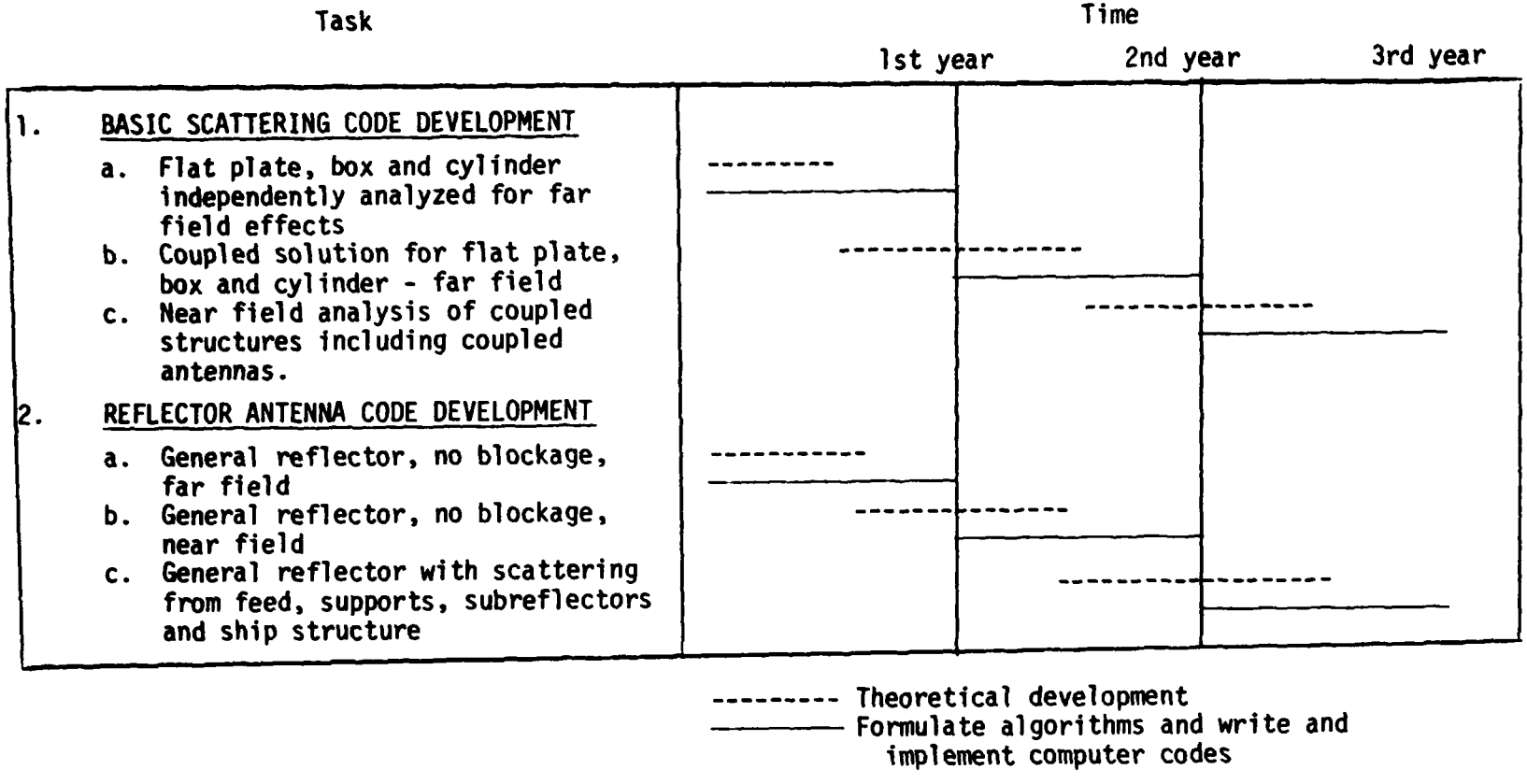

Table I. Milestone chart for total program.

TABLE II

ASYMPTOTIC HIGH FREQUENCY TECHNIQUES
FOR UHF AND ABOVE ANTENNAS

FIRST YEAR WORK PLAN

Topic	1st Quarter Task	2nd Quarter Task
1. Basic Scattering Code Development		
	FF Flat Plate (T,A)	FF Box (T,A)
	FF Cylinder (T,A)	FF Cylinder (T,A)
2. Reflector Antenna Code Development		
	General reflector	General reflector
	FF w/o blockage (T)	FF w/o blockage (T)
3. Theoretical Studies		
	Slope Diffraction (T)	Vertex Diffraction (T)

T - Theory

A - Algorithm

U - Code with User's Manual

TABLE II (Contd.)

ASYMPTOTIC HIGH FREQUENCY TECHNIQUES
FOR UHF AND ABOVE ANTENNAS

FIRST YEAR WORK PLAN

Topic	3rd Quarter Task	4th Quarter Task
1. Basic Scattering Code Development		
	FF Box (A,U)	FF Box (U)
	FF Cylinder (A,U)	FF Cylinder (U)
Plate, Box, Cylinder	Coupled FF (T,A)	Coupled FF (T,A)
2. Reflector Antenna Code Development		
	General Reflector FF w/o blockage (T,A)	General Reflector FF w/o blockage (A,U)
	General Reflector NF w/o blockage (T)	General Reflector NF w/o blockage (T)
3. Theoretical Studies		
	Vertex Diffraction (T)	Vertex Diffraction (T)

A newly developed multiple plate scattering code used to model wing-mounted aircraft antennas [1] facilitates the use of separate flat plates to form a box shape. This multiplate code allows a number of N sided flat plates to be placed in proximity to each other such that they can be defined with common edges. The solution as originally developed, however, included the scattering mechanisms that best approximated aircraft wing geometries. Necessary modifications are being made to the code so that arbitrary box-shaped structures can be handled. The comparison of the GTD result for a dipole antenna near two plates forming a convex edge are presented in Figure 1 to illustrate the present state of the solution. The GTD result is compared with a reaction method result (moment method solution) in this figure to show the validity of the result.

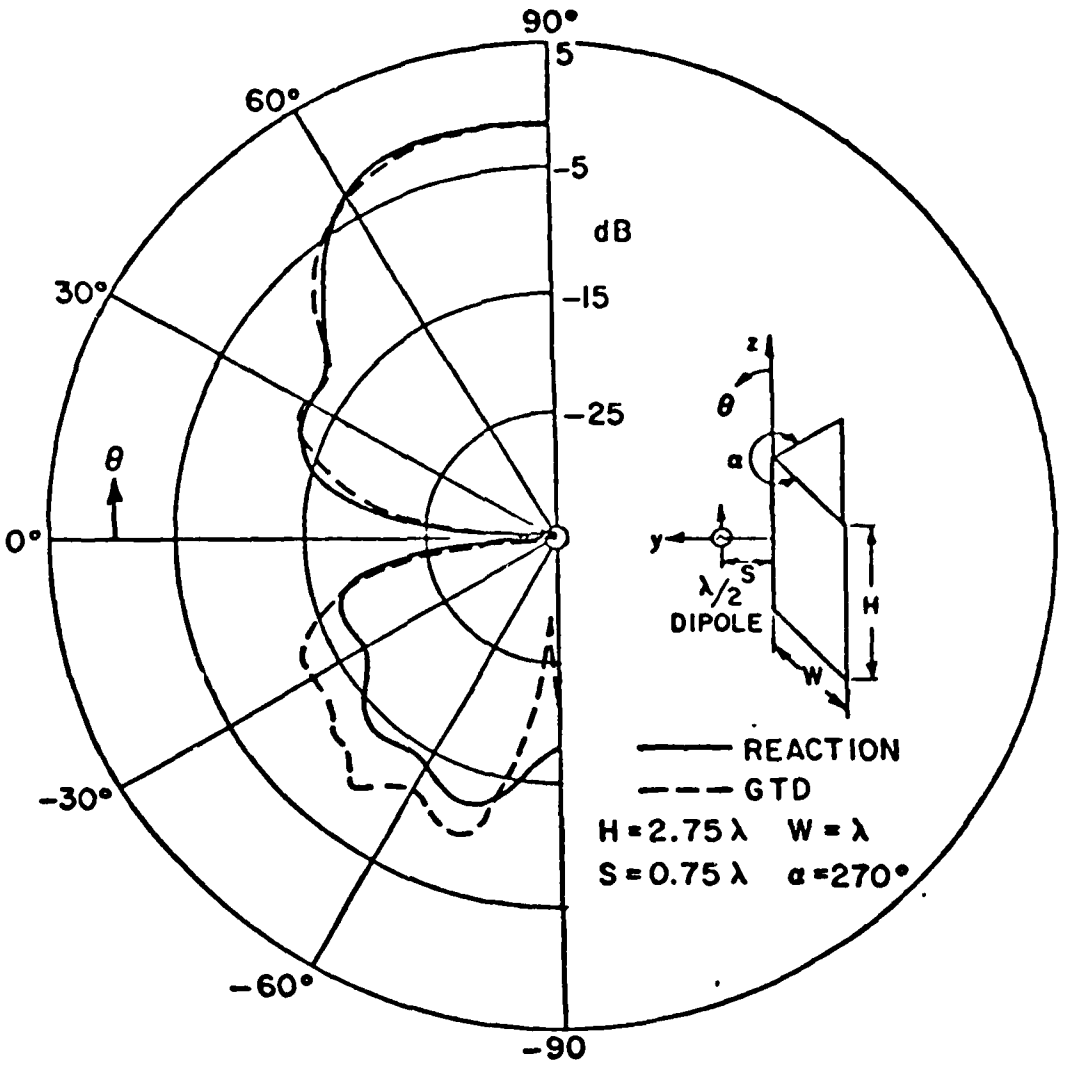

Figure 1. Comparison of reaction and GTD E-plane pattern results (α=270°).

In connection with the theoretical effort of this contract, the importance of using the dyadic slope diffraction term in the scattering code is illustrated in Figure 2 for a slot on a flat plate. An empirical corner diffraction coefficient that will be used initially is also under study at this time. To illustrate the importance of this diffraction mechanism for flat plate structures, a comparison of a result with and without the corner diffraction term is shown in Figure 3. The validity of this solution is shown by comparing against a measured result in Figure 4. The agreement is very good even though the corner term is empirical.

The overall efficiency of the basic scattering code is also under investigation. It will be important to make the scattering code work as accurately and efficiently as possible for individual antenna elements since eventually a large number of elements will be needed in conjunction with the moment method (AMP code, etc.) solution for wire antenna structures.

The above mentioned investigations have prepared the way for an easy transition of the flat plate scattering code to handle box-like shapes. It should also be noted that certain parts of the flat plate scattering code also can be applied to the general reflector antenna problem. The applicable methods developed for the flat plate will be modified so that they can be used to model the edges of the general parabolic dish problem. This will allow the analysis of the fields in the shadow region (behind the reflector) in which the feed is not visible.

In a parallel effort, our finite elliptic cylinder scattering code for aircraft is also under investigation. In particular, the diffraction mechanisms used to model the junction between the flat plate endcaps and the curved elliptic cylinder surface is presently under study. A curved edge dyadic diffraction coefficient is used to find the field scattered from the edges. Also, an equivalent current method under development on another program will be used to correct for problems in the caustic regions of the curved edges. The present form of these results, however, have been relatively inefficient. A means of making these terms numerically more efficient will be investigated in the next period.

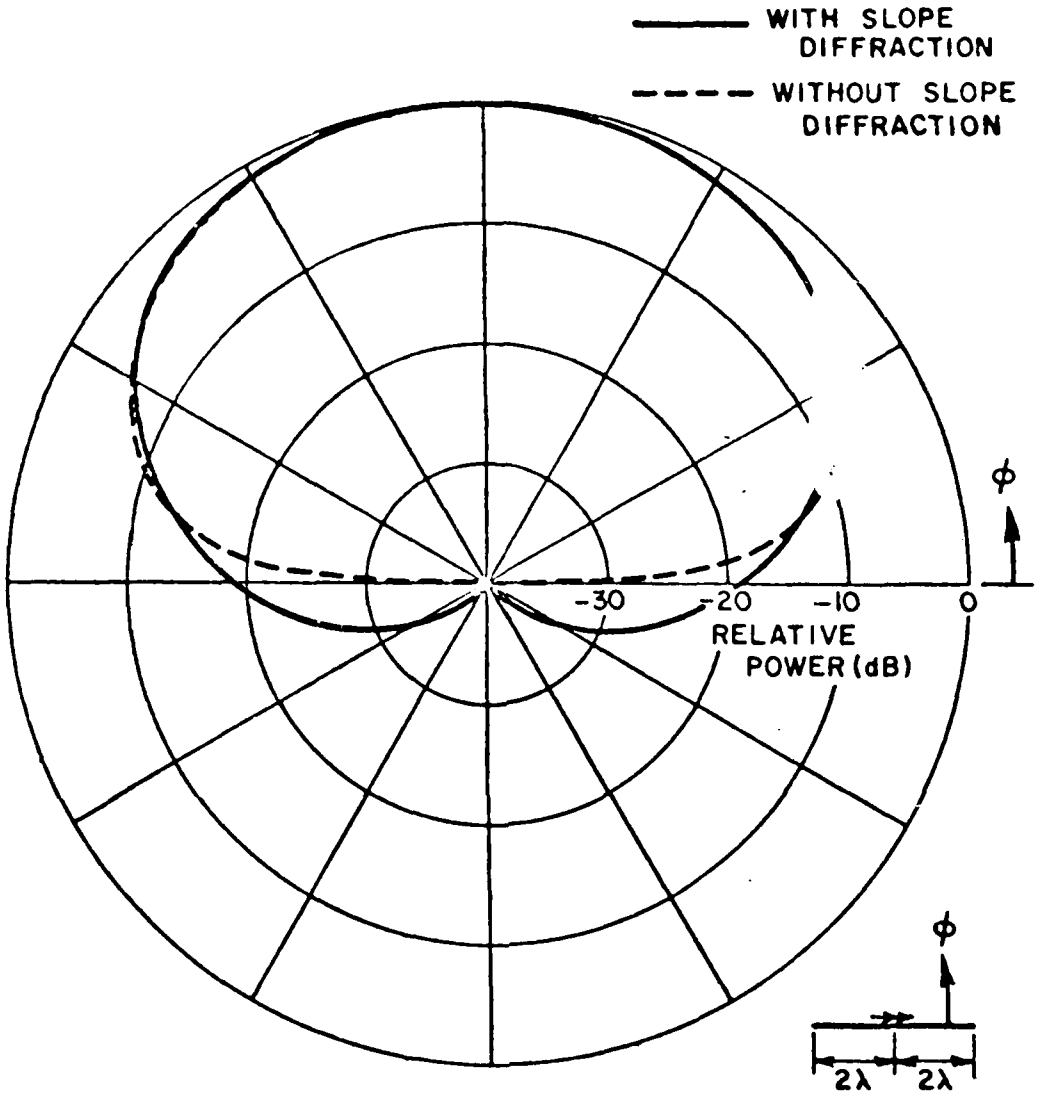

Figure 2. Comparison of the E_θ radiation pattern of a strip slot on a plate with and without slope diffraction.

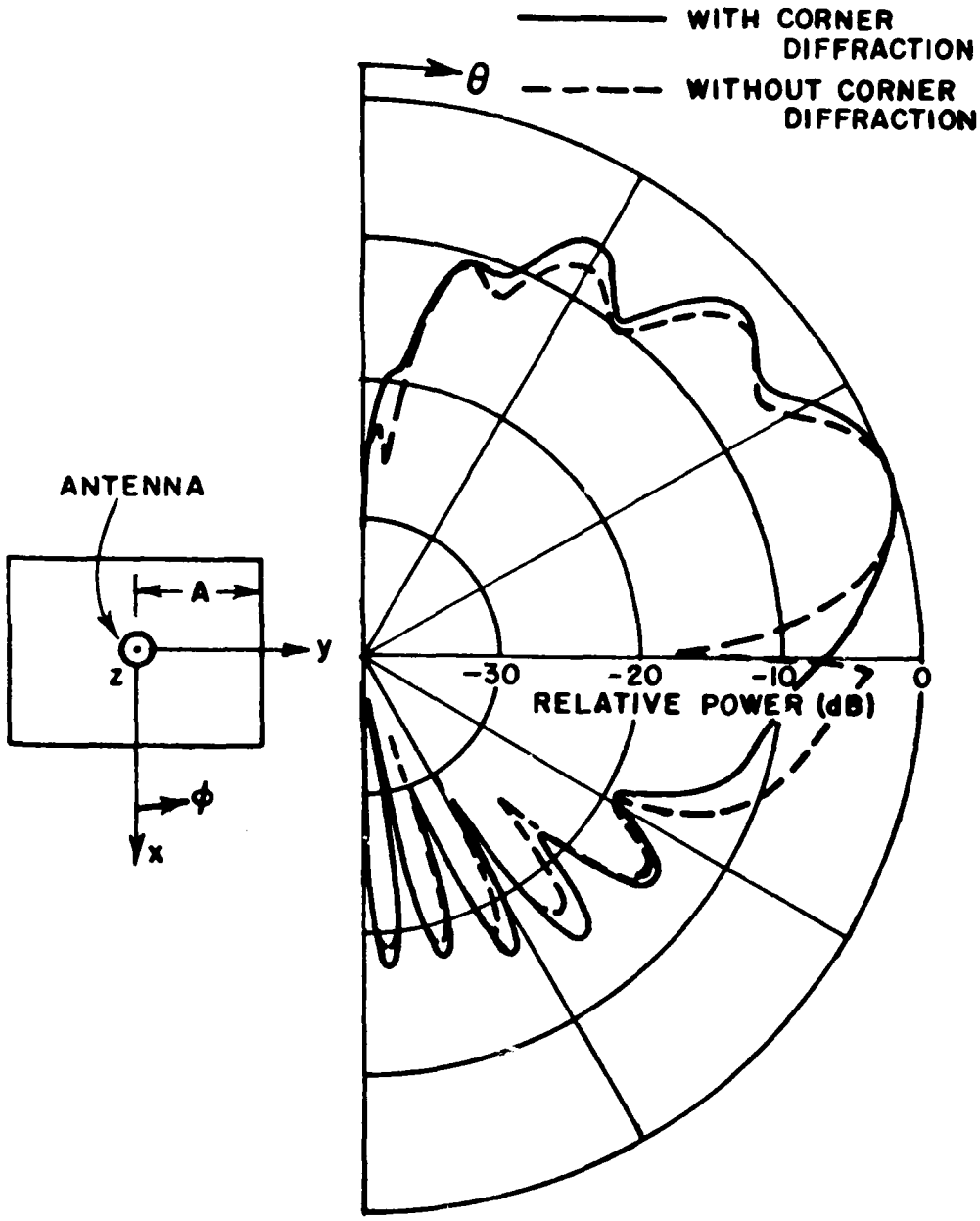

Figure 3. Comparison of the E_θ radiation pattern of a short monopole on a square plate (A=4λ) with or without corner diffraction taken in the plane ϕ=45°.

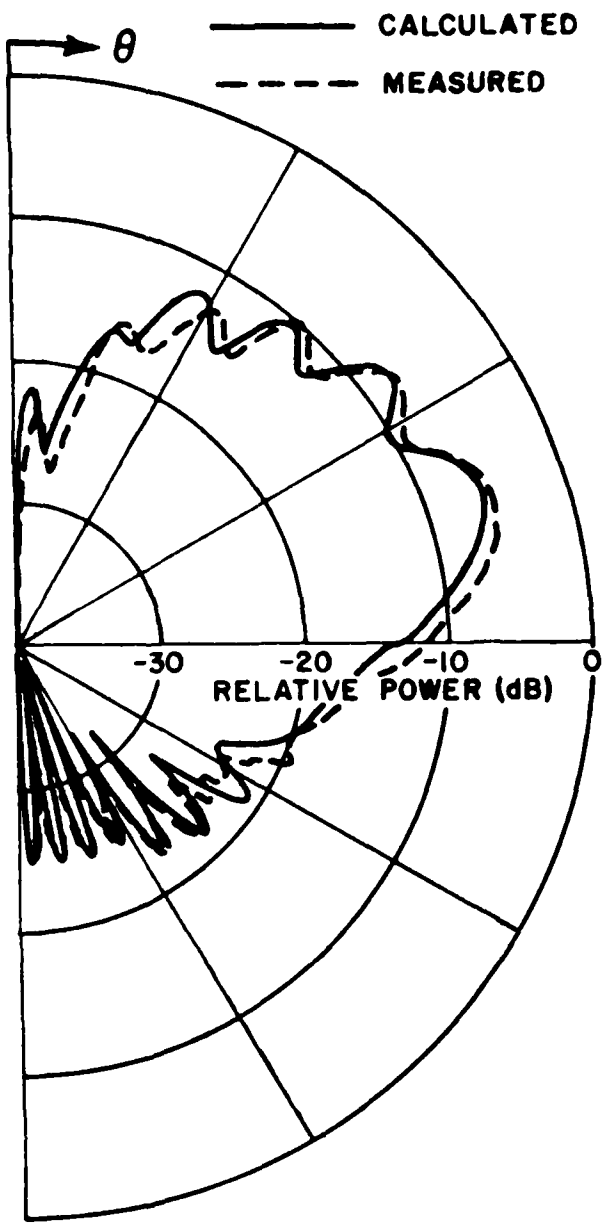

Figure 4. Comparison of the calculated and measured E_θ radiation pattern of a short monopole on a square plate ($A=5.51\lambda$) taken in the plane $\phi=45°$.

IV. REFLECTOR ANTENNA CODE DEVELOPMENT

The purpose of the present effort is to develop a user-oriented computer program package by which the far field pattern of a typical Navy reflector antenna can be calculated. Feed blockage and scattering effects are not included in this phase. These will be included later (see Table I).

The theoretical approach for computing the far field pattern of the general reflector is based on a combination of the Geometrical Theory of Diffraction (GTD) and Aperture Integration (AI) techniques. AI will be used to compute the main beam and near sidelobes; GTD will be used to compute the wide-angle sidelobes and the backlobes. To implement the computer algorithms based on these theories, efficient ways are needed to handle calculations involving the feed pattern and the reflector geometry. It is planned to treat the geometry of the reflector rim by using best-fit elliptical or linear segments.

Since the majority of Navy reflector antennas have parabolic surfaces, only the class of parabolic surfaces will be implemented in the computer code. The code for the reflector geometry will be flexible enough to include off-set fed reflectors and general reflector rim shapes such as elliptical and rectangular with chopped corners.

An efficient way to handle the feed pattern is necessary because of the time-consuming nature of the AI calculations for electrically large reflectors. Fortunately, AI is needed only for the main beam and near sidelobe regions of the pattern. GTD is very efficient for calculating most of the pattern. A promising way to treat the feed pattern is to use a polynomial fit for each measured pattern cut of the volumetric feed pattern. This method provides a computationally efficient way of calculating the aperture field without requiring large amounts of computer storage for the measured feed pattern. Only relatively few coefficients need to be stored for essentially complete feed pattern information. Furthermore, the polynomial-fit method has the advantages of flexibility and simplicity for general feed patterns. No cut-and-try procedures are needed; the polynomial coefficients can be computed automatically from the measured feed pattern input.

A computer subroutine has been developed to test the accuracy of the polynomial-fit method for feed patterns. An arbitrary number of measured feed pattern values may be used as input for this subroutine. The subroutine will then calculate the polynomial fit for the specified feed data with an exact fit at the measured points. This method for approximating the feed pattern has been tested thusfar on a typical sum pattern and a typical difference pattern. The result is shown in Figure 5 for the sum pattern with a fit at five pattern points:

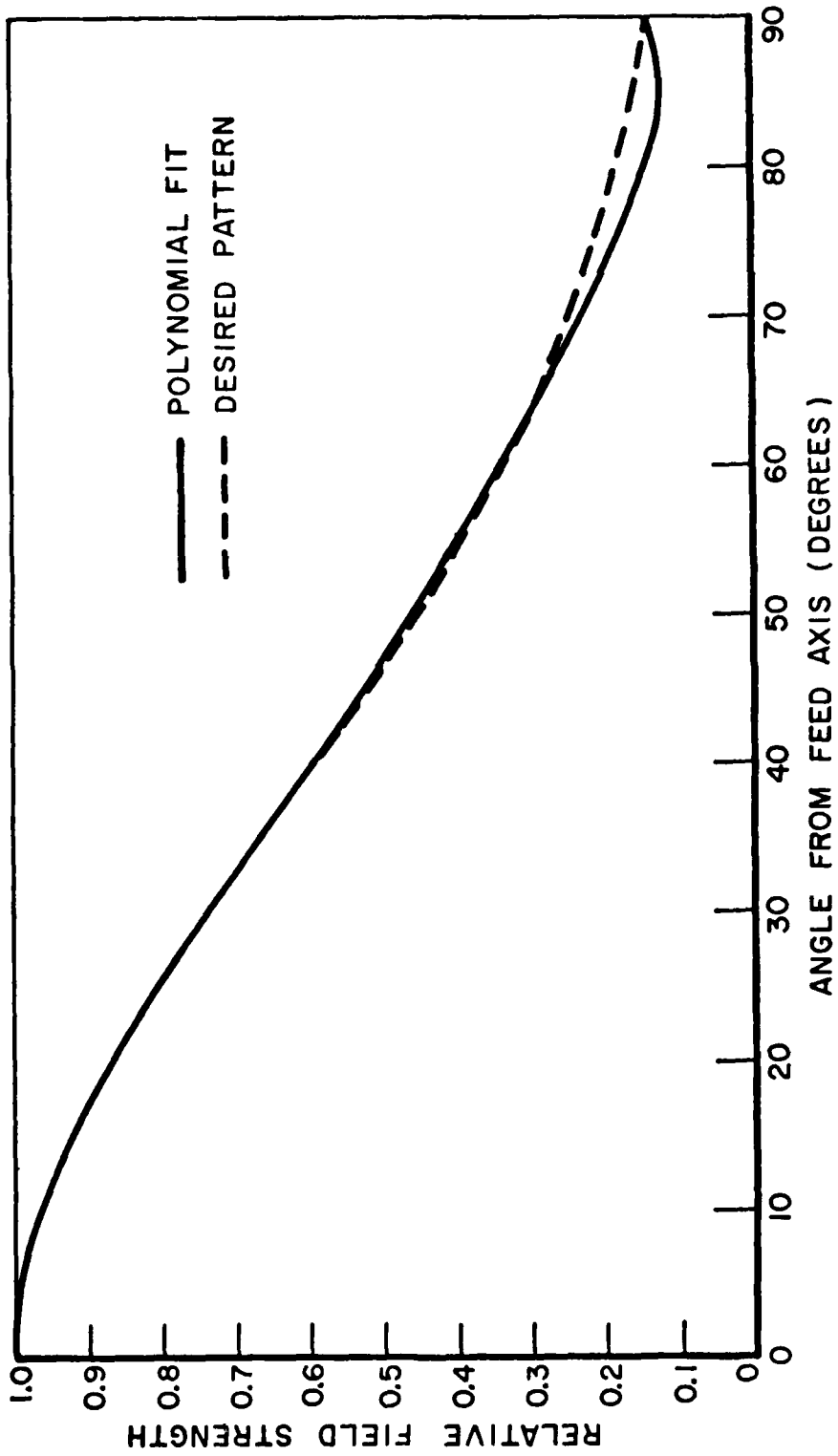

Figure 5. Polynomial fit for typical feed sum pattern. Exact fit at 0°,10°,30°,60°,90°.

0°, 10°, 30°, 60°, 90°. The difference pattern in Figure 6 was fitted at six points: 0°, 10°, 20°, 30°, 40°, 50°. As can be seen, these results are very accurate except at low feed pattern levels which will not significantly affect the accuracy of the AI computations.

During the next Quarter, a suitable numerical technique for AI will be established. This includes developing the detailed theory for ray tracing to establish the aperture field and the numerical integration to compute the main beam and near sidelobe pattern of the general reflector.

V. THEORETICAL STUDIES

A uniform solution for the diffraction of an electromagnetic wave by a perfectly-conducting wedge has been obtained within the format of the geometrical theory of diffraction. The total high frequency field is the sum of the geometrical optics field and an edge diffracted field. Since the geometrical optics field is discontinuous at shadow and reflection boundaries, the diffracted field must provide a compensating discontinuity so that the total field and its derivatives are continuous there. In addition, the diffracted field must provide the proper transition between the illuminated and shadow regions of the incident and reflected fields.

If the field incident on the edge does not have a rapid spatial variation, the diffracted field is directly proportional to the incident field at the edge; it can be calculated using the dyadic diffraction coefficient given by Kouyoumjian and Pathak [2]. In the proper ray-fixed coordinate system this diffraction coefficient is merely the sum of two dyads. Represented as a matrix, the diffraction coefficient is a 2x2 diagonal matrix. The diagonal elements are D_h and D_s, the acoustic hard and soft scalar diffraction coefficients, which contain Fresnel integrals so that they may be used in the transition regions. This diffraction coefficient can be used for both curved and ordinary wedge geometries.

What happens when the incident field has a rapid spatial variation at the edge? If the edge diffracted field is calculated in the usual way, using the Kouyoumjian Pathak diffraction coefficient, there will be a discontinuity in the spatial derivatives of the total field, i.e., the calculated pattern will be continuous but have a "kink" in it. A simple example of this is a wedge illuminated by a dipole line source so that the electric field $E^i(Q_E)$ incident at its edge vanishes. The geometry of this two dimensional problem is depicted in Figure 7. The diffracted electric field $E^d(s)$ neglecting slope diffraction is given by

$$E^d(s) = E^i(Q_E) D_s(\phi,\phi') \frac{e^{-jks}}{\sqrt{s}} \quad . \qquad (1)$$

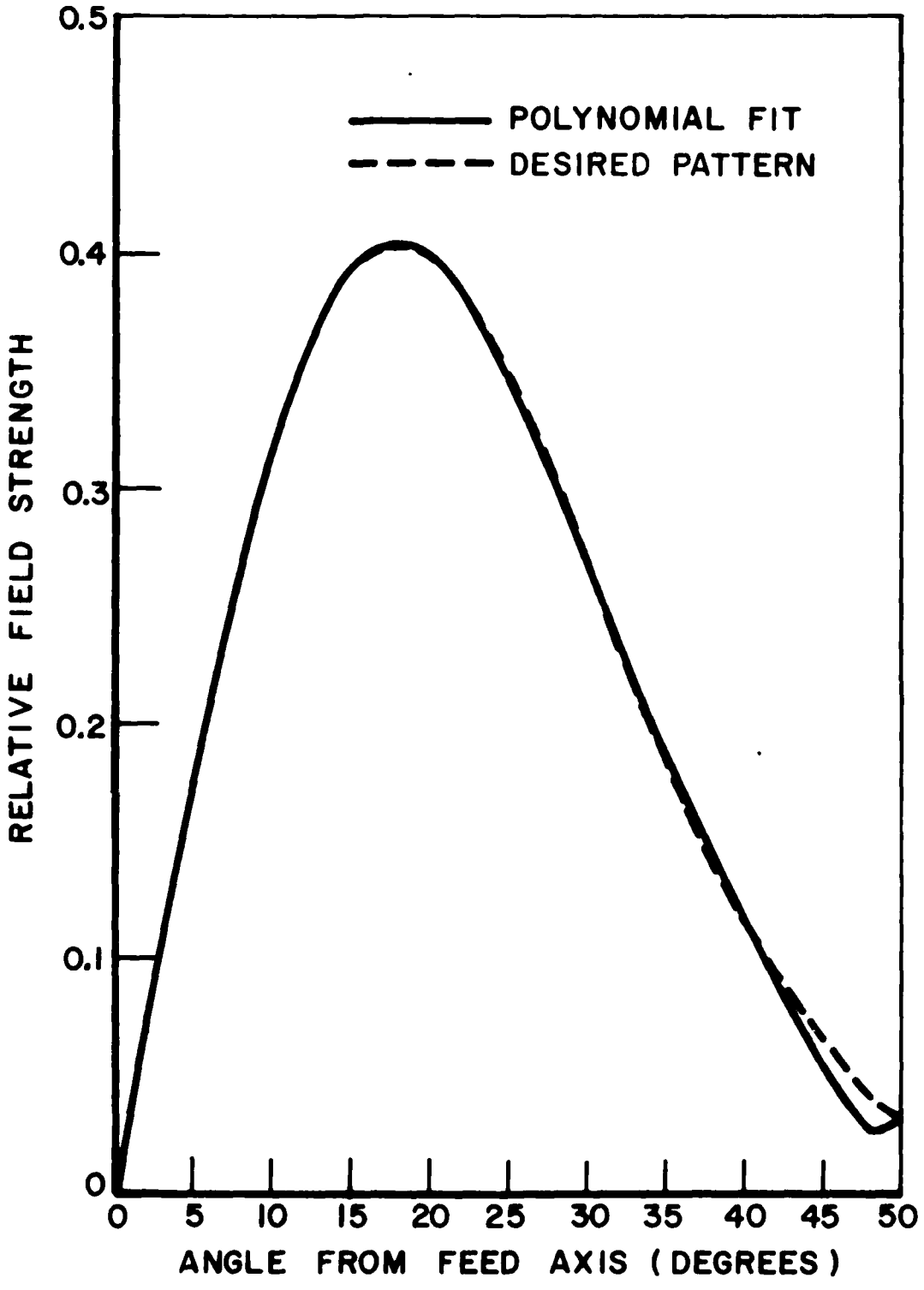

Figure 6. Polynomial fit for typical feed difference pattern. Exact fit at 0°,10°,20°,30°,40°,50°.

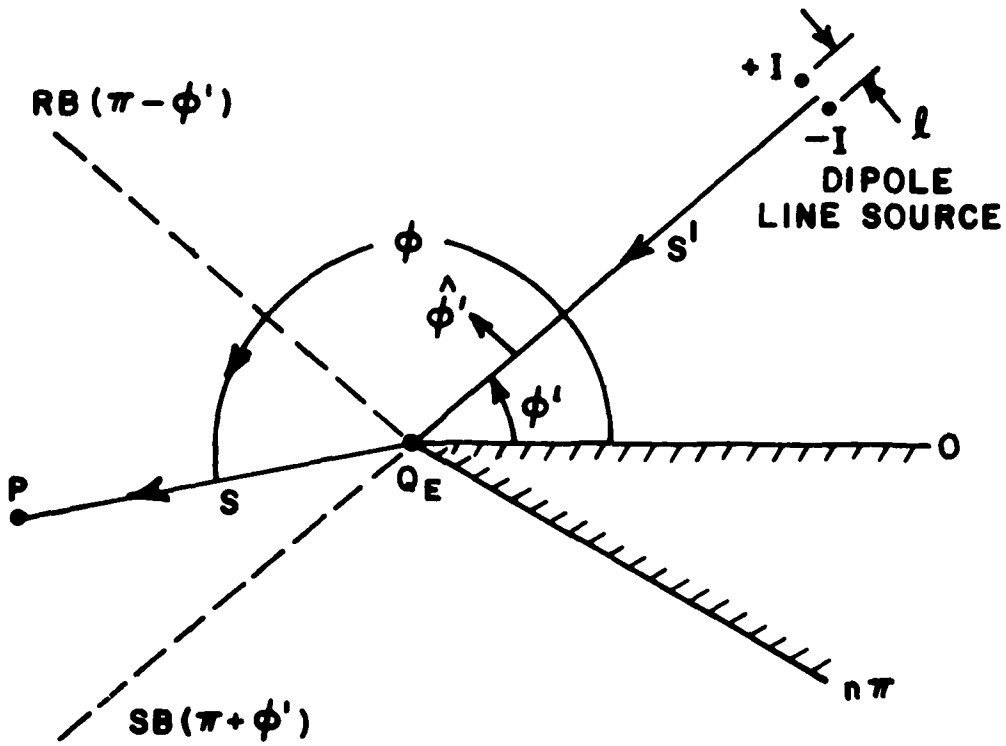

Figure 7. Wedge illuminated by a line source dipole.

Since $E^i(Q_E) = 0$, it is apparent that $E^d(s) = 0$, and the total high frequency electric field is the geometrical optics field, whose far-zone pattern function is

$$\sin(\phi-\phi')H(\pi+\phi'-\phi)e^{jks'\sin\phi'\sin\phi} + \sin(\phi+\phi')H(\pi-\phi'-\phi)e^{-jks'\sin\phi'\sin\phi} \quad , \qquad (2)$$

$$0 \leq \phi \leq n\pi \quad ; \quad 0 \leq \phi' < \pi ,$$

where $$H(x) = \begin{cases} 1, & x > 0 \\ 0, & x < 0 \end{cases} \qquad (3)$$

is the unit step function and $0 \leq \phi \leq n\pi$.

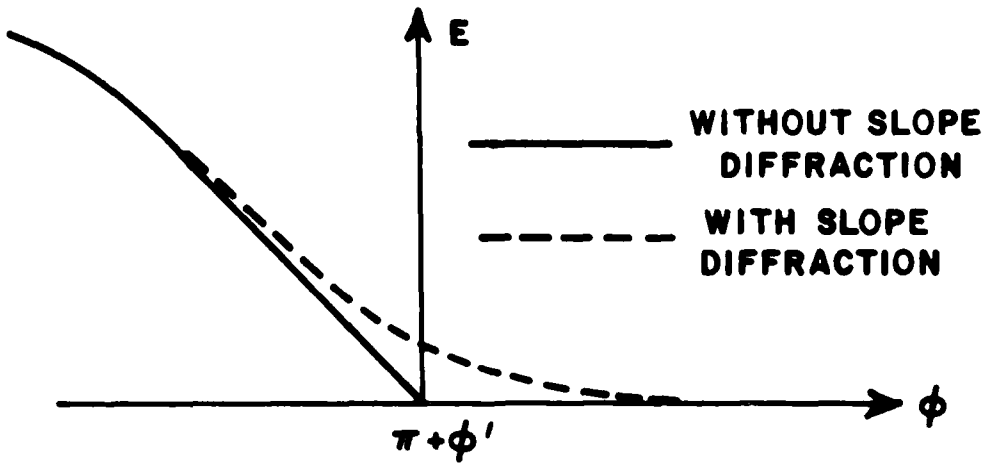

Figure 8. Far zone total field near the shadow boundary.

It is evident that the total high frequency field is continuous at the shadow and reflection boundaries at $\phi = \pi + \phi'$ and $\pi - \phi'$, respectively, but that its derivative with respect to ϕ is not. Thus there is a "kink" in the pattern function as illustrated in Figure 8. Actually the diffracted field does not vanish as implied by Equation (1); it depends upon the spatial derivative of the incident field taken in the direction of $\hat{\phi}'$, i.e., normal to the edge-fixed plane of incidence (this is the plane for which $\phi = \phi'$). Employing the slope diffraction term

$$E^d(s) = \frac{\partial E^i(Q_E)}{\partial n} \left[\frac{1}{jk} \frac{\partial}{\partial \phi'} D_s(\phi, \phi') \right] \frac{e^{-jks}}{\sqrt{s}} , \qquad (4)$$

where the bracketed term is referred to as the slope diffraction coefficient. In an alternate approach, Kouyoumjian has shown that the above expression can be obtained from the ordinary diffracted field of each line source treated separately. Equation (4) results when the diffracted fields of the two line sources are superimposed and the limit taken as their separation ℓ vanishes (the dipole strength $I\ell$ remains bounded). When the contribution from Equation (4) is included in the pattern calculation, the pattern has the form shown by the dotted curve in Figure 8. It is seen that the total field and its derivatives are now continuous at the shadow boundary. The total diffracted field is the sum of the ordinary contribution from Equation (1) and the higher-order, slope contribution from Equation (4); outside the transition regions it can be shown that the former is of order $k^{-1/2}$, whereas the latter is of order $k^{-3/2}$.

A dyadic slope diffraction coefficient for an electromagnetic wave obliquely incident on a perfectly-conducting wedge has been derived by Kouyoumjian and Hwang [3,4]. Two methods were employed. In the first approach they asymptotically solved a canonical problem, where the electric and magnetic current dipole sources are parallel to the ray incident at the point of diffraction on the edge. Since the incident field vanishes at the point of diffraction, only the higher-order slope diffracted field remains, as in the case of the dipole line source problem considered earlier. In the second approach the field incident at the edge is decomposed into a sum of inhomogeneous plane waves. The edge diffraction for each of these waves is determined, and the diffracted field is then synthesized from these components, one of which is the slope diffraction term.

The slope diffraction term and its relationship to the ordinary term is given below with the ordinary and slope diffraction coefficients written in matrix form:

$$\begin{bmatrix} E^d_{\beta_o} \\ E^d_{\phi} \end{bmatrix} = \left\{ \begin{bmatrix} -D_s & 0 \\ 0 & -D_h \end{bmatrix} \begin{bmatrix} E^i_{,\beta_o} \\ E^i_{\phi'} \end{bmatrix} + \begin{bmatrix} -d_s & 0 \\ 0 & -d_h \end{bmatrix} \begin{bmatrix} \frac{\partial}{\partial n} E^i_{,\beta_o} \\ \frac{\partial}{\partial n} E^i_{\phi'} \end{bmatrix} \right\} x$$

$$x \sqrt{\frac{\rho}{s(\rho+s)}} \; e^{-jks} \quad , \tag{5}$$

where

$$d_{s,h} = \frac{1}{jk\sin\beta_o} \frac{\partial}{\partial \phi'} D_{s,h} \; . \tag{6}$$

The partial derivative with respect to distance n is taken in the direction normal to the edge-fixed plane of incidence and ρ is the distance between the point of diffraction on the edge and the second caustic of the tube of diffracted rays. Figure 9 serves to explain the remaining notation. Although this figure depicts curved edges and curved surfaces, it is still helpful in the present discussion, since one may regard the wedge as a special case of the curved edge structure.

As pointed out in [2] the first term makes the total high-frequency field continuous at shadow and reflection boundaries, whereas the second (or slope diffraction) term makes the first partial derivatives of the total high-frequency field continuous at these boundaries. Work is under way to extend the present slope diffraction analysis for the wedge to the curved wedge.

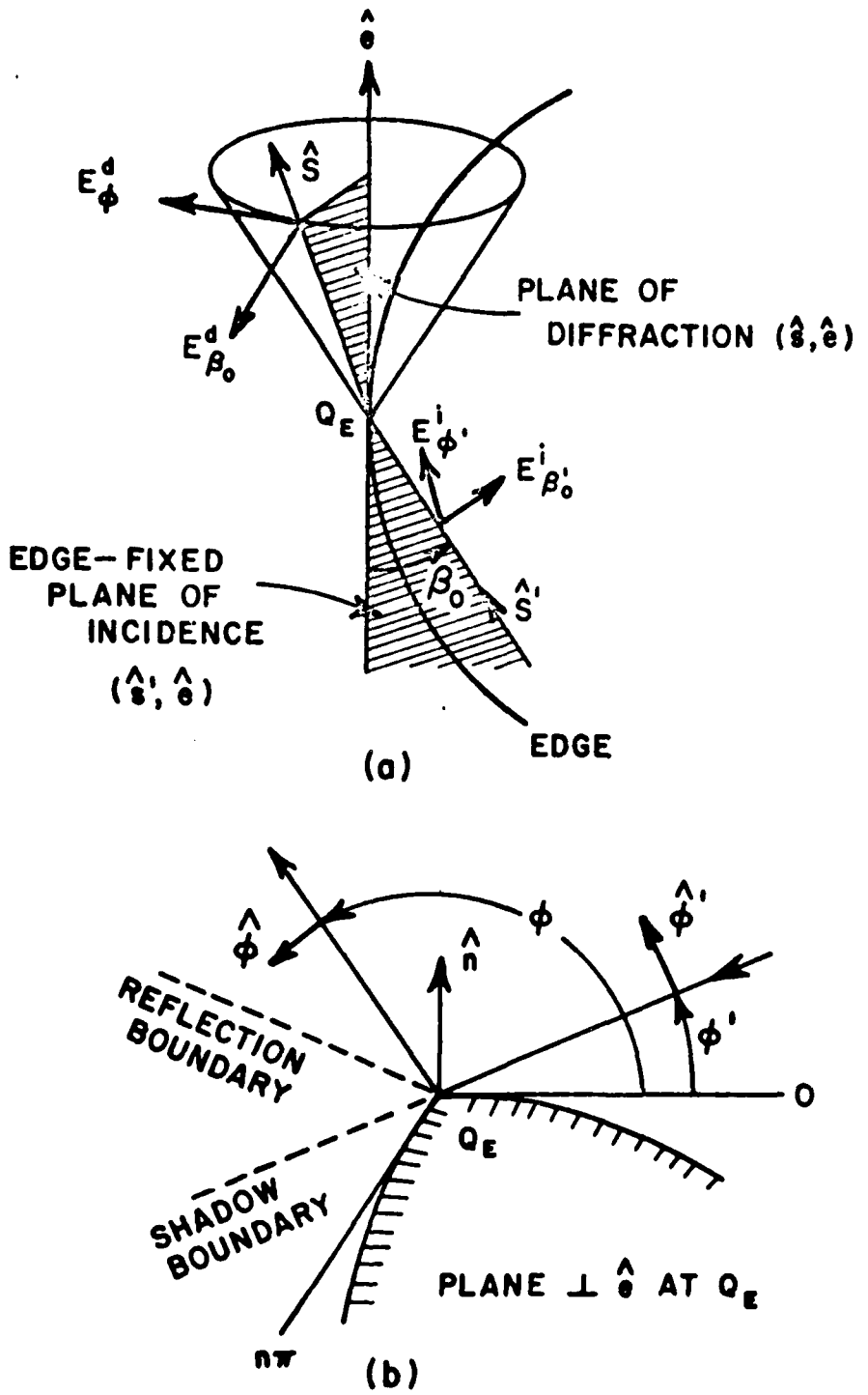

Figure 9. Diffraction at an edge.

We conclude this section by considering an example which demonstrates the accuracy of the present slope diffraction analysis. Consider the radiation from an infinitesimal slot positioned perpendicular to the edge of a perfectly-conducting right angle wedge as shown in Figure 10. Let us calculate the pattern in a plane perpendicular to the edge.

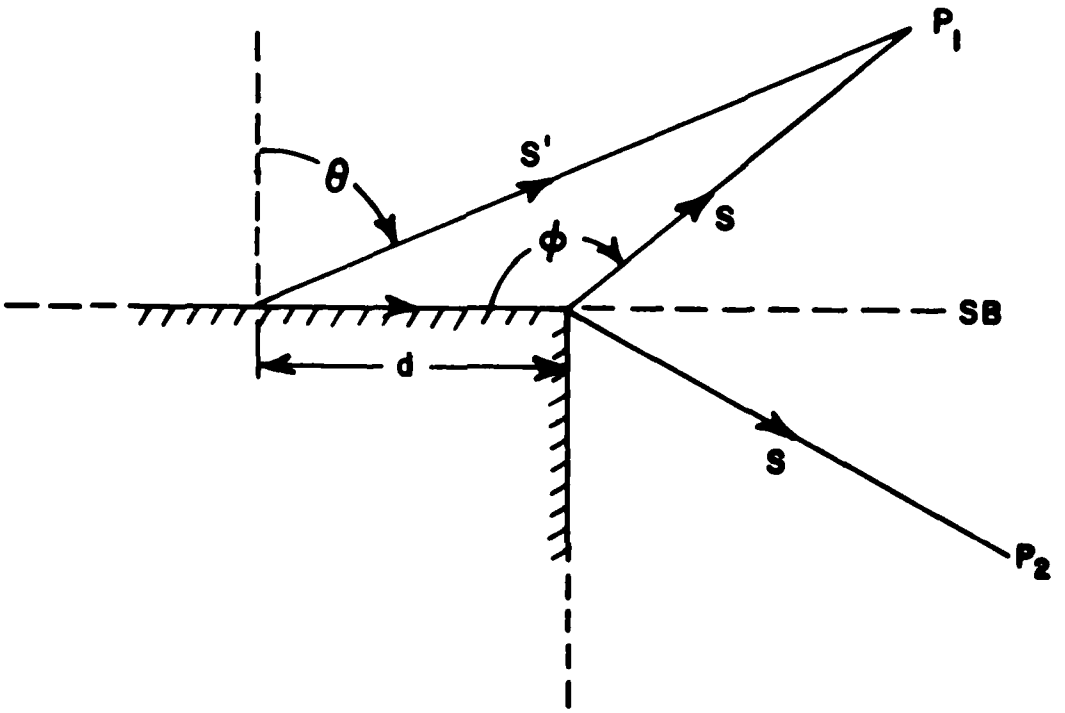

Figure 10. A slot on a right angle wedge. Slot is perpendicular to edge and distance d from edge.

The geometrical optics field is

$$E^{go} = \begin{cases} A \dfrac{e^{-jks'}}{s'} \cos\theta , & 0 \leq \phi < \pi \\ 0 , & \pi < \phi \leq \dfrac{3\pi}{2} . \end{cases} \qquad (7)$$

Employing Equations (5) and (6), the diffracted field is

$$E^d = \frac{\partial}{\partial n} E^i \left[\frac{1}{2jk} \frac{\partial}{\partial \phi'} D_s(\phi,\phi') \right] \Bigg|_{\phi'=0} \sqrt{\frac{d}{s(d+s)}}\, e^{-jks} \qquad (8)$$

in which $\frac{\partial}{\partial n} E^i = \frac{A}{d^2} e^{-jkd}$,

and the factor of 1/2 is introduced into the expression for the slope diffraction coefficient because of grazing incidence.

The far-zone patterns calculated from GTD and eigenfunction (exact) solutions are compared in Figure 11. In this case the slot is only $\lambda/8$ away from the edge; nevertheless, the agreement between the two patterns is seen to be excellent. This agreement is even more impressive when one considers that the solution depends upon the derivative of the ordinary diffraction coefficient D_s. If the Kouyoumjian-Pathak expression for this diffraction coefficient were not extremely accurate, there would be noticeable differences between the GTD and "exact" patterns. These differences would be particularly noticeable in the shadow region, where only the diffracted field exists. The GTD solution becomes increasingly accurate as d/λ increases; however, even for d/λ as small as .05, the GTD solution is no more than one or two dB in error in the deep shadow region. Also as d/λ increases, the field at the shadow boundary diminishes rapidly, so that for $d/\lambda = 1$ it is -16 dB with respect to the geometrical optics, incident field. A similar example of the application of slope diffraction has been given earlier in Section III, see Figure 2.

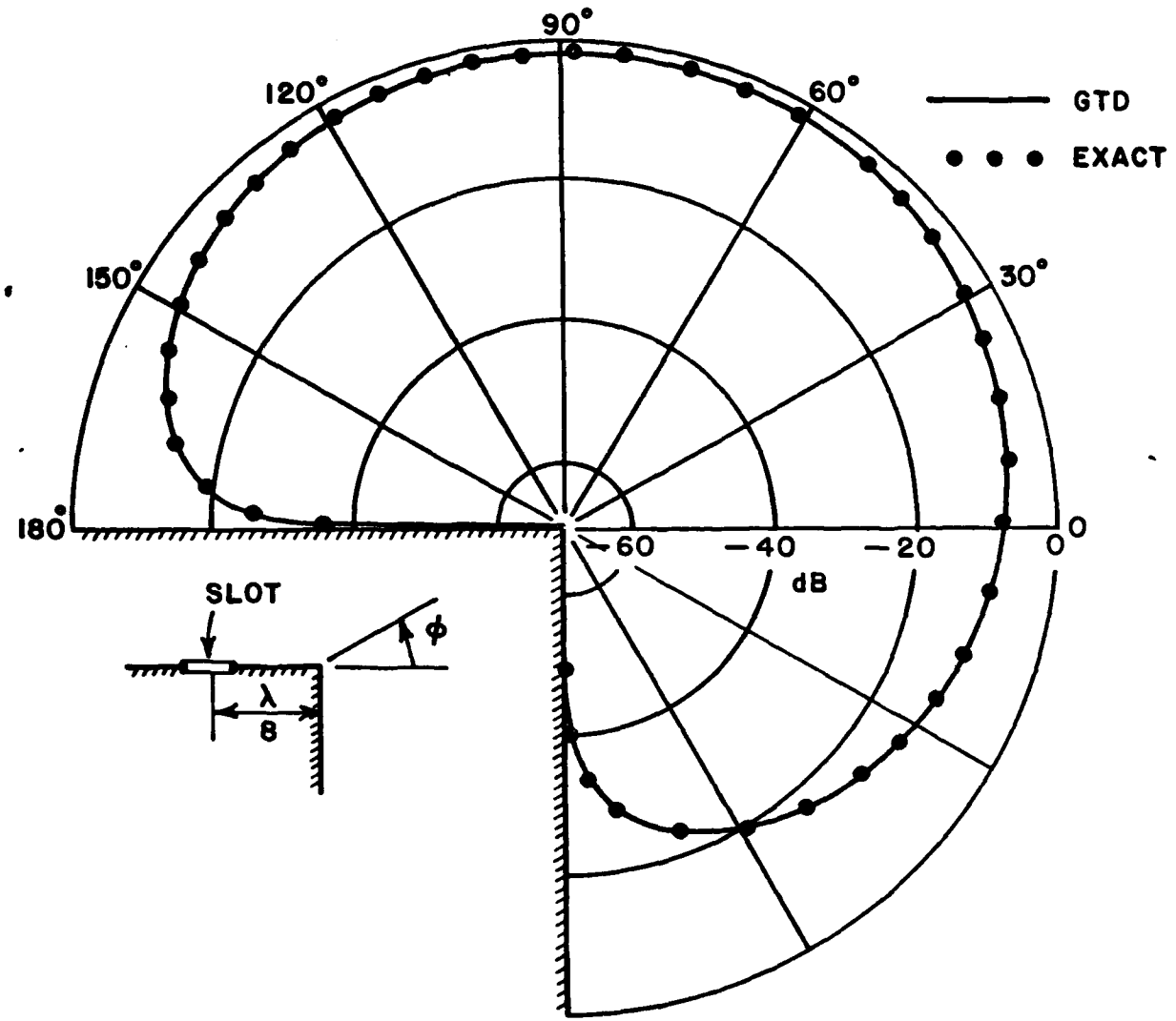

Figure 11. Pattern of a slot on a right angle wedge (slot perpendicular to edge).

REFERENCES

[1] R. J. Marhefka, "Analysis of Aircraft Wing-Mounted Antenna Patterns," Report 2902-25, June 1976, The Ohio State University ElectroScience Laboratory, Department of Electrical Engineering; prepared under Grant No. NGL 36-008-138 for National Aeronautics and Space Administration.

[2] R. G. Kouyoumjian and P. H. Pathak, "A Uniform Geometrical Theory of Diffraction for an Edge in a Perfectly Conducting Surface," Proc. IEEE, Vol. 62, November 1974, pp. 1448-1461.

[3] Y. M. Hwang and R. G. Kouyoumjian, "A Dyadic Diffraction Coefficient for an Electromagnetic Wave Which is Rapidly Varying at an Edge," USNC-URSI 1974 Annual Meeting, Boulder, Colorado, October 1974.

[4] Y. M. Hwang and R. G. Kouyoumjian, "On the Dyadic Slope Diffraction Coefficient," USNC-URSI Meeting, Urbana, Illinois, June 1975.